

B-Raf Acts via the ROCKII/LIMK/Cofilin Pathway To Maintain Actin Stress Fibers in Fibroblasts

Catrin A. Pritchard,^{1*} Louise Hayes,^{2†} Leszek Wojnowski,³ Andreas Zimmer,⁴
Richard M. Marais,² and Jim C. Norman¹

Department of Biochemistry, University of Leicester, Leicester LE1 7RH,¹ and Institute of Cancer Research, London SW3 6JB,² United Kingdom, and Department of Pharmacology, Johannes Gutenberg University, D-55101 Mainz,³ and Molekulare Neurobiologie, Klinik und Poliklinik für Psychiatrie und Psychotherapie, 53105 Bonn,⁴ Germany

Received 18 July 2003/Returned for modification 13 September 2003/Accepted 8 March 2004

Recent data have shown that the *BRAF* gene is mutated at a high frequency in human malignancies. We have analyzed the migratory characteristics of *B-raf*^{-/-} mouse embryonic fibroblasts (MEFs) and compared these with the organization of the actin cytoskeleton and the activity of signaling pathways that are known to influence this organization. Disruption of *B-raf* significantly reduced the levels of phospho-ERK1/2 and, surprisingly, induced an ≈1.5-fold increase in cell migration. Consistent with these findings, the high level of actin stress fibers normally present in MEFs was considerably reduced following disruption of *B-raf*, and the F-actin content of *B-raf*^{-/-} cells was less than half that of *B-raf*^{+/+} cells. Phosphorylation of the myosin light chain on Thr18/Ser19 residues was not reduced in *B-raf*^{-/-} cells. Rather, reduced ROCKII expression and attenuated phosphorylation of ADF/cofilin on serine 3 occurred. Normal stress fiber and phosphocofilin levels were restored by the expression of human B-Raf and catalytically active MEK and by the overexpression of LIM kinase (LIMK). These results have important implications for the role of the B-Raf/ERK signaling pathway in regulating cell motility in normal and malignant cells. They suggest that B-Raf is involved in invasiveness by regulating the proper assembly of actin stress fibers and contractility through a ROCKII/LIMK/cofilin signaling pathway.

Members of the Raf family of serine/threonine protein kinases have been well studied in a variety of organisms ranging from *Drosophila* to humans. Three *raf* homologues (*raf-1*, *B-raf*, and *A-raf*) exist in mammals, while a single prototypic homologue exists in lower organisms. A wealth of genetic and biochemical data have indicated that Raf family members are signaling kinases that are integral components of the conserved Ras/Raf/MEK/ERK signaling cascade. Following activation by Ras-dependent mechanisms, Raf protein kinases act as mitogen-activated protein (MAP) kinase kinase kinases, which phosphorylate and activate the type 1/2 MAP kinase kinases, also known as MEK1/2. These dual-specificity threonine and tyrosine kinases in turn phosphorylate and activate the ERK1/2 members of the MAP kinase family. This highly conserved Ras/Raf/MEK/ERK pathway serves to relay signals from the extracellular membrane to cellular effectors and has a profound influence on cell fate by regulating patterns of proliferation, differentiation, apoptosis, and motility (7, 25).

All three mammalian Raf proteins have been shown to bind to MEK1/2 and lead to the sequential activation of MEK and ERK in vitro (12, 24, 33). However, there is accumulating evidence that B-Raf may be the more important physiological MEK activator. When endogenous Raf isoforms were immunoprecipitated and their activities were measured by using the MEK/ERK kinase cascade assay, B-Raf was shown to have

considerably stronger kinase activity than the other two isoforms (14, 16). B-Raf is known to have a higher affinity for MEK1 than Raf-1 (29) and also to have a higher level of basal activity toward its substrate (24, 26). Gene targeting studies have shown that ERK phosphorylation and activation are not disrupted in mice or mouse embryonic fibroblasts (MEFs) containing an *A-raf* knockout mutation (27), a *raf-1* knockout mutation (14, 28), or a MEK kinase-inactive version of Raf-1 with the Y340FY341F mutation (14). However, preliminary studies of *B-raf*^{-/-} MEFs have shown that ERK phosphorylation is significantly reduced, if not absent, following stimulation with epidermal growth factor (EGF) (40).

The appropriate regulation of the phosphorylation status and activity of the ERKs, as imposed by the Ras/Raf/MEK pathway, is absolutely critical to maintaining cell homeostasis (39). If ERK activity is inappropriately regulated, then cell transformation can arise (4), leading to tumorigenesis (6, 13). Oncogenic Ras alleles are detected in over 30% of human cancers (3) and are thought, at least in part, to mediate their effects through the deregulation of ERK activation (8). Activating mutations of the *BRAF* gene were detected recently in 70% of human malignant melanomas (6), 30% of thyroid cancers (18), and 15% of colon cancers. A total of 82% of *BRAF* mutations encode the V599E mutant, which has basal kinase activity 12.5-fold higher than wild-type B-Raf activity and stimulates constitutive ERK phosphorylation (6). Oncogenic *BRAF* and *RAS* alleles are rarely present in the same cancer samples, but they are present in the same cancer types and are thought to transform cells in a similar way through their ability to induce constitutive ERK phosphorylation (6).

While the function of ERKs has been best characterized

* Corresponding author. Mailing address: Department of Biochemistry, University of Leicester, University Rd., Leicester LE1 7RH, United Kingdom. Phone: 44 116 2523489. Fax: 44 116 2525097. E-mail: cap8@le.ac.uk.

† Present address: GlaxoSmithKline, Marlow, Essex CM19 5AW, United Kingdom.

with regard to their ability to translocate to the nucleus and phosphorylate transcription factor complexes, ERKs also have a number of cytoplasmic substrates that can influence cell growth (39), apoptosis (20), and motility (2). With regard to cell motility, Klemke et al. (19) showed that the phosphorylation of myosin light chain (MLC₂₀) kinase (MLCK) is high in cells expressing constitutively active MEK but is reduced in cells treated with MEK inhibitors (9, 19). MLCK also contains multiple MAP kinase consensus phosphorylation sites, and both ERK1 and ERK2 are able to directly phosphorylate MLCK, leading to enhanced MLCK activity. MLCK-mediated phosphorylation of serine 19 and threonine 18 of MLC is critical in myosin function, since it promotes myosin ATPase activity and the contractility of actomyosin. Consistent with these findings, it has been shown that ERK is involved in the potentiation of force development in vascular smooth muscle, most likely through the regulation of MLCK (5). ERK-mediated MLCK or myosin potentiation may also be important for targeting active ERK to newly formed focal adhesions (9).

The expression of oncogenic alleles in fibroblasts is associated with MEK/ERK-dependent disruption of the actin cytoskeleton (30, 31, 35, 42). The sustained activation of ERK induced by oncogenic Ras leads to posttranscriptional down-regulation of the expression of ROCK1 and Rho kinase (ROCKII), two Rho effectors required for actin stress fiber formation (31, 35). This down-regulation leads to reduced signaling through the LIM kinase (LIMK)/cofilin pathway but is functionally restored by MEK inhibition or by the overexpression of ROCK (31, 35). Similarly, *v-src*-induced disruption of the actin cytoskeleton of fibroblasts is mediated by sustained MEK/ERK signaling and leads to the down-regulation of ROCK expression and dephosphorylation of the actin-depolymerizing protein cofilin (30).

In order to begin to assess how deregulated B-Raf activity may contribute to the motile phenotype of normal and tumor cells, we have analyzed MEFs derived from mice bearing a null mutation for *B-raf* (40, 41). These *B-raf*^{-/-} mice die in mid-gestation at embryonic day 12.5 (E12.5) due to increased levels of spontaneous apoptosis of the endothelial cell lineage. However, the phenotype of *B-raf*^{-/-} MEFs derived from these mice has not been investigated to date. Our studies now show that the most profound defect is one of altered motility associated with a collapsed actin cytoskeleton. *B-raf*^{-/-} cells have significantly reduced levels of ERK1/2 phosphorylation. Contrary to what might be expected from the suggested role of ERK in controlling MLCK activity (19), however, the levels of phospho-MLC are not significantly changed. Instead, we provide evidence for a role of B-Raf in regulating a ROCKII/LIMK/cofilin signaling pathway leading to actin polymerization.

MATERIALS AND METHODS

Derivation and culturing of MEFs. Mice containing a heterozygous knockout mutation of the *B-raf* gene were described previously (41). These mice were backcrossed onto the C57BL/6 genetic background. To obtain *B-raf*^{-/-} MEFs and sibling control *B-raf*^{+/+} MEFs, female and male *B-raf*^{+/-} mice were intercrossed. Embryos were collected at E12.5 and homogenized, and fibroblasts were grown from the embryos by standard procedures (14, 32). Each primary MEF culture was isolated from a single embryo. For PCR genotyping, a tail sample was taken from each embryo prior to homogenization. This sample was lysed for 2 h in lysis buffer (50 mM KCl, 10 mM Tris-HCl [pH 8.3], 2.5 mM MgCl₂, 0.1 μg of gelatin/ml, 0.45% [vol/vol] NP-40, 0.45% Tween 20, 200 μg of fresh proteinase

K/ml) at 55°C. Samples were heat inactivated at 95°C for 10 min and subjected to PCR. PCR was performed with primers and conditions described previously (41). Fibroblasts were cultured in low-glucose (1.0 g/liter) Dulbecco's modified Eagle's medium (DMEM) (Life Technologies) containing 10% (vol/vol) fetal calf serum (FCS) (SeraQ) and 100 U of penicillin-streptomycin (Life Technologies)/ml in a 10% CO₂ humidified incubator at 37°C. Primary cell cultures were immortalized by the 3T3 method.

B-Raf kinase assays. Immortalized cells were made quiescent by culturing in DMEM containing 0.5% (vol/vol) FCS for 20 h. They were stimulated by the addition of 10 ng of EGF/ml for various times. Protein lysates were prepared as described by Marais et al. (24). B-Raf was immunoprecipitated for 2 h at 4°C from 0.1 mg of lysate with 4 μg of an anti-B-Raf rabbit polyclonal antibody (26). The activity of each Raf protein was assessed and quantitated as described by Marais et al. (24).

Cell stimulation and immunoblotting. For the ERK and cofilin phosphorylation assays, primary MEFs were serum starved for 30 min and then stimulated either with 10 ng of EGF/ml over a time course of 0 to 60 min or with 50 ng of platelet-derived growth factor (PDGF)/ml, 40 μM phorbol myristate acetate (PMA), 200 ng of lysophosphatidic acid (LPA)/ml, or 10% (vol/vol) FCS for 10 min. For all other assays, cells were grown to confluence and refed with serum-containing DMEM prior to lysis. Preparation of protein lysates, Western blotting, and Coomassie blue staining were carried out as described previously (22).

Primary antibodies were as follows: a 1:1,000 dilution of a mouse monoclonal antibody for Thr202/Tyr204 phospho-p44/42 ERK (Cell Signaling Technologies), a 1:1,000 dilution of a rabbit polyclonal antibody for ERK2 (Zymed Laboratories Inc.), a 1:1,000 dilution of vinculin monoclonal antibody F9 (a gift from V. Kotliansky, Centre National de la Recherche Scientifique, Paris, France), a 1:1,000 dilution of an antibody for actin (Sigma), a 1:250 dilution of a mouse monoclonal antibody for ROCK1 (BD Transduction Laboratories), a 1:1,000 dilution of a mouse monoclonal antibody for ROCKII (BD Transduction Laboratories), a 1:500 dilution of a rabbit polyclonal antibody for Thr18/Ser19 phospho-MLC (Santa Cruz Biotechnology Inc.), a 1:5,000 dilution of a mouse monoclonal antibody for MLC₂₀ (Sigma), a 1:5,000 dilution of a rabbit polyclonal antibody for Ser3 phospho-ADF/cofilin (a gift from Jim Bamburg, Colorado State University), a 1:1,000 dilution of a rabbit polyclonal antibody for ADF/cofilin (a gift from Alan Weeds, University of Cambridge), and a 1:1,000 dilution of a mouse monoclonal antibody for B-Raf (Santa Cruz Biotechnology).

Detection of the antigen-antibody complexes was performed as described previously with the appropriate secondary antibodies (22).

Wounding and transmigration assays. For wounding assays, primary MEFs were plated on 3-cm tissue culture plates coated with 10 μg of fibronectin/ml and allowed to grow until confluent. With a pipette tip, crosses were scraped into the confluent monolayers. Cells were washed with phosphate-buffered saline (PBS), refed with serum-containing complete medium, and allowed to grow at 37°C. Photographs of the wounds were taken at 0, 4, 6, 9, 12, 16, and 24 h postwounding. To obtain a quantitative estimate of migration following wounding, the cell-free area contained within each 466-μm linear stretch of wound (the equivalent of a photographic field) was determined by using NIH Image software.

For transmigration assays, Boyden chamber assays were used. The lower surfaces of 24-well cell culture inserts supporting an 8-μm-pore-size polycarbonate membrane (Life Technologies) in 24-well plates were coated with 25 μg of fibronectin/ml overnight at 4°C. The inserts were washed with PBS and transferred to new 24-well plates. To the lower chamber, 400 μl of complete growth medium was added. A total of 2.5 × 10⁵ cells in 400 μl of serum-free medium were added to the upper chamber, and the cells were allowed to migrate at 37°C for 5 h. The upper surfaces of the chambers then were wiped with a cotton bud to remove nonmigratory cells. Migratory cells on the lower surfaces then were fixed with 10% (wt/vol) paraformaldehyde in PBS for 30 min at room temperature. Cells were washed with PBS three times before being stained with 1% (wt/vol) toluidine blue in PBS for 1 h at room temperature. To remove excess stain, chambers were washed extensively with water and air dried, and the dye was extracted from the cells with 500 μl of 2% (wt/vol) sodium dodecyl sulfate (SDS). The absorbance at 630 nm was measured. Each assay was performed three times in triplicate for each primary cell line.

Immunofluorescence. Coverslips were sterilized and coated with 25 μg of fibronectin/ml in PBS overnight. A total of 10⁵ cells in serum-containing complete medium were used to seed coverslips, which were left overnight in a 37°C incubator. The medium was aspirated, and the cells were fixed with 2% (wt/vol) paraformaldehyde in PBS for 10 to 20 min at room temperature. Cells were washed with PBS and then permeabilized with 0.2% (vol/vol) Triton X-100 in PBS for 2 to 5 min at room temperature. Cells were washed with PBS and then blocked with 1% (wt/vol) bovine serum albumin (BSA) in PBS for 1 h. A total of

100 μ l of primary antibody diluted in 1% BSA (wt/vol) in PBS was applied, and the cells were incubated for 1 h at room temperature.

Primary antibodies were as follows: a 1:500 dilution of a paxillin antibody (BD Transduction Laboratories), a 1:100 dilution of vinculin monoclonal antibody F9, a 1:1,000 dilution of a rabbit polyclonal antibody for ERK2, a 1:100 dilution of a rabbit polyclonal antibody for Thr18/Ser19 phospho-MLC (a gift from M. Crow, Johns Hopkins University, Baltimore, Md.), a 1:100 dilution of a rabbit polyclonal antibody for Ser217/Ser221 phospho-MEK (Cell Signaling Technologies), a 1:100 dilution of a rabbit antibody for the hemagglutinin (HA) tag (Santa Cruz Biotechnology), and a 1:100 dilution of a mouse monoclonal antibody for the Myc tag (clone 9E10; Santa Cruz Biotechnology).

Cells were washed for at least 20 min with PBS and then were incubated with a 1:100 dilution of the appropriate fluorescein isothiocyanate (FITC)-coupled secondary antibody in 1% (wt/vol) BSA in PBS for 1 h at room temperature. Cells were washed again for at least 20 min with PBS and then incubated with a 1:100 dilution of phalloidin-Texas Red in PBS for 20 min. Cells were washed extensively and then mounted in ProLong antifade mounting reagent (Molecular Probes) prior to fluorescence microscopy.

Determination of cell surface integrin expression. MEFs grown to 80 to 90% confluence were refed with fresh DMEM containing 10% FCS. After 30 min, the MEFs were washed and surface labeled with 0.2 mg of NHS-S-S-biotin/ml for 30 min at 4°C. The MEFs were lysed in 100 μ l of a buffer containing 200 mM NaCl, 75 mM Tris, 15 mM NaF, 1.5 mM Na_3VO_4 , 7.5 mM EDTA, 7.5 mM EGTA, 1.5% Triton X-100, 0.75% Igepal CA-630, 50 μ g of leupeptin/ml, 50 μ g of aprotinin/ml, and 1 mM 4-(2-aminoethyl)benzenesulfonyl fluoride and were scraped from the dish with a rubber policeman. Lysates were passed three times through a 27-gauge needle and clarified by centrifugation at $10,000 \times g$ for 10 min. Supernatants were corrected to equivalent protein concentrations, and levels of biotinylated integrin were determined by a capture enzyme-linked immunosorbent assay as follows.

Maxisorb 96-well plates (Life Technologies) were coated overnight with 5 μ g of rat anti-mouse $\alpha 5$ integrin (clone 5H10-27 [MFR5])/ml or 5 μ g of hamster anti-mouse $\beta 3$ integrin (clone 2C9.G2) (both from Pharmingen, San Diego, Calif.) in 0.05 M Na_2CO_3 (pH 9.6) at 4°C. Nonspecific binding sites were blocked with PBS containing 0.05% (vol/vol) Tween 20 (PBS-T) and 5% BSA for 1 h at room temperature. Integrins were captured by overnight incubation of 50 μ l of cell lysate at 4°C. Unbound material was removed by extensive washing with PBS-T, and wells were incubated with streptavidin-conjugated horseradish peroxidase in PBS-T containing 1% BSA for 1 h at 4°C. Following further washing, biotinylated integrins were detected by a chromogenic reaction with 0.56 mg of *ortho*-phenylenediamine/ml in a buffer containing 25.4 mM Na_2HPO_4 , 12.3 mM citric acid (pH 5.4), and 0.003% (vol/vol) H_2O_2 at room temperature for 10 min. The reaction was stopped with 8 M H_2SO_4 , and the absorbance at 490 nm was measured. The integrity of the captured material was checked by SDS-6% PAGE under nonreducing conditions; this step was followed by Western blotting and detection with streptavidin-conjugated horseradish peroxidase and chemiluminescence.

Analysis of cell spreading. Twelve-well tissue culture plates (Life Technologies) were coated with fibronectin (F-1141; Sigma) or vitronectin (V-8379; Sigma) at a concentration of 20 μ g/ml overnight at 4°C. The wells were rinsed with PBS and subsequently blocked with 2% (wt/vol) BSA in PBS for 2 h at room temperature. MEFs were harvested by trypsinization and collected by centrifugation in the presence of 20 μ g of soybean trypsin inhibitor/ml. Cell suspensions in medium containing 10 ng of PDGF-BB/ml or in serum-containing complete medium were added immediately to ligand-coated wells. Cells were allowed to attach for 30 min or 1 h. Nonadherent cells were removed by six washes with PBS, and attached cells were fixed for 10 min with 4% (wt/vol) paraformaldehyde in PBS. To obtain an index of cell spreading, adherent cells were photographed with a digital camera, and their areas were determined by delineation of the cell envelope and calculation of the encompassed area by using NIH Image software.

Transfection of MEFs. Immortalized MEFs were transfected with a vector expressing HA-tagged full-length LIMK (a gift from Gordon Gill, University of California at San Diego), Myc-tagged full-length human B-Raf, catalytically active MEK1 (CA-MEK) with the S217E and S221E mutations (a gift from Chris Marshall, ICR, London, United Kingdom), or green fluorescent protein (GFP). A total of 10^6 B-*raf*^{-/-} immortalized MEFs were transfected with each vector by using a Nucleofector under the MEF conditions recommended by the manufacturer (Amaxa Biosystems, Cologne, Germany). At 24 or 48 h following transfection, cells in serum-containing complete medium were used to seed fibronectin-coated coverslips and were processed for immunofluorescence.

Quantitation of F-actin levels. Confluent cells of each primary MEF cell line on three 10-cm plates were harvested and washed with PBS. Cell pellets were fixed with 8% (wt/vol) paraformaldehyde in PBS for 10 min at room tempera-

ture. Cells were washed three times with PBS and permeabilized with 0.3% (vol/vol) Triton X-100 in PBS for 1 min at room temperature. Following three washes with PBS, cells were stained with 0.6 μ M FITC-phalloidin in PBS for 10 min at room temperature. Cells were washed three times with PBS and then analyzed by fluorescence-activated cell sorting (FACS) (Becton Dickinson).

RESULTS

Generation of B-*raf*^{-/-} MEFs. Embryos were harvested from B-*raf*^{+/-} intercross litters, and primary MEFs were derived from each embryo (see Materials and Methods). Genotypes of each cell line were confirmed by PCR analysis of embryo tail DNA, a typical example of which is shown in Fig. 1A. For all experiments, at least three different B-*raf*^{-/-} clones were compared to three different B-*raf*^{+/+} clones. Western blot analysis with a B-Raf-specific antibody was used to confirm the absence of full-length and truncated B-Raf proteins in B-*raf*^{-/-} MEFs (Fig. 1B). In addition, a B-Raf kinase immunocomplex assay was performed. B-*raf*^{-/-} and B-*raf*^{+/+} immortalized MEFs were serum starved and then stimulated with EGF over a time course of 0 to 60 min. Protein lysates were harvested and used in a B-Raf kinase immunocomplex assay as described previously (24) (see Materials and Methods). As expected, no B-Raf kinase activity was detected in B-*raf*^{-/-} MEFs (Fig. 1C). Similar results were obtained when two other B-Raf antibodies were used for immunoprecipitation (data not shown).

Levels of phospho-ERK1/2 are significantly reduced in B-*raf*^{-/-} MEFs. A previous study showed that there is little, if any, phospho-ERK1/2 in B-*raf*^{-/-} MEFs following stimulation with EGF for 10 min (40). To perform a more extensive study of ERK phosphorylation in these cells, we used Western blot analysis to compare the levels of phospho-ERK1/2 following stimulation with a wider variety of extracellular stimuli. B-*raf*^{-/-} and B-*raf*^{+/+} MEFs were serum starved and then stimulated with EGF over a time course of 0 to 30 min. Protein lysates were generated, electrophoresed by SDS-PAGE, Western blotted, and analyzed with an antibody for Thr202/Tyr204 phospho-p44/42 ERK. As a control for protein loading, blots were also analyzed with an antibody for ERK2. A typical example of data obtained for one set of MEFs is shown in Fig. 2A. Consistent with previous data, phospho-ERK1/2 levels in B-*raf*^{-/-} cells were significantly lower than phospho-ERK1/2 levels in B-*raf*^{+/+} cells.

MEFs were also serum starved and then stimulated with serum (Fig. 2B), LPA (Fig. 2C), or PMA (Fig. 2D) for 0 to 30 min, and phospho-ERK1/2 levels were analyzed. For all stimuli, phospho-ERK levels were lower in B-*raf*^{-/-} cells than in B-*raf*^{+/+} cells. There was no significant difference in the time course of ERK phosphorylation following stimulation, except upon PMA treatment of the cells, with which the induction of ERK phosphorylation appeared to be delayed. We also attempted to study ERK phosphorylation following plating of cells kept in suspension on fibronectin. However, we consistently failed to observe any induction of ERK phosphorylation under these conditions, even in B-*raf*^{+/+} cells (data not shown). There was also no significant difference in the induction of phosphorylation of ERK1 versus ERK2.

This analysis of ERK1/2 phosphorylation was repeated several times for different sets of MEFs following treatment with various stimuli. On all occasions, we found greatly reduced

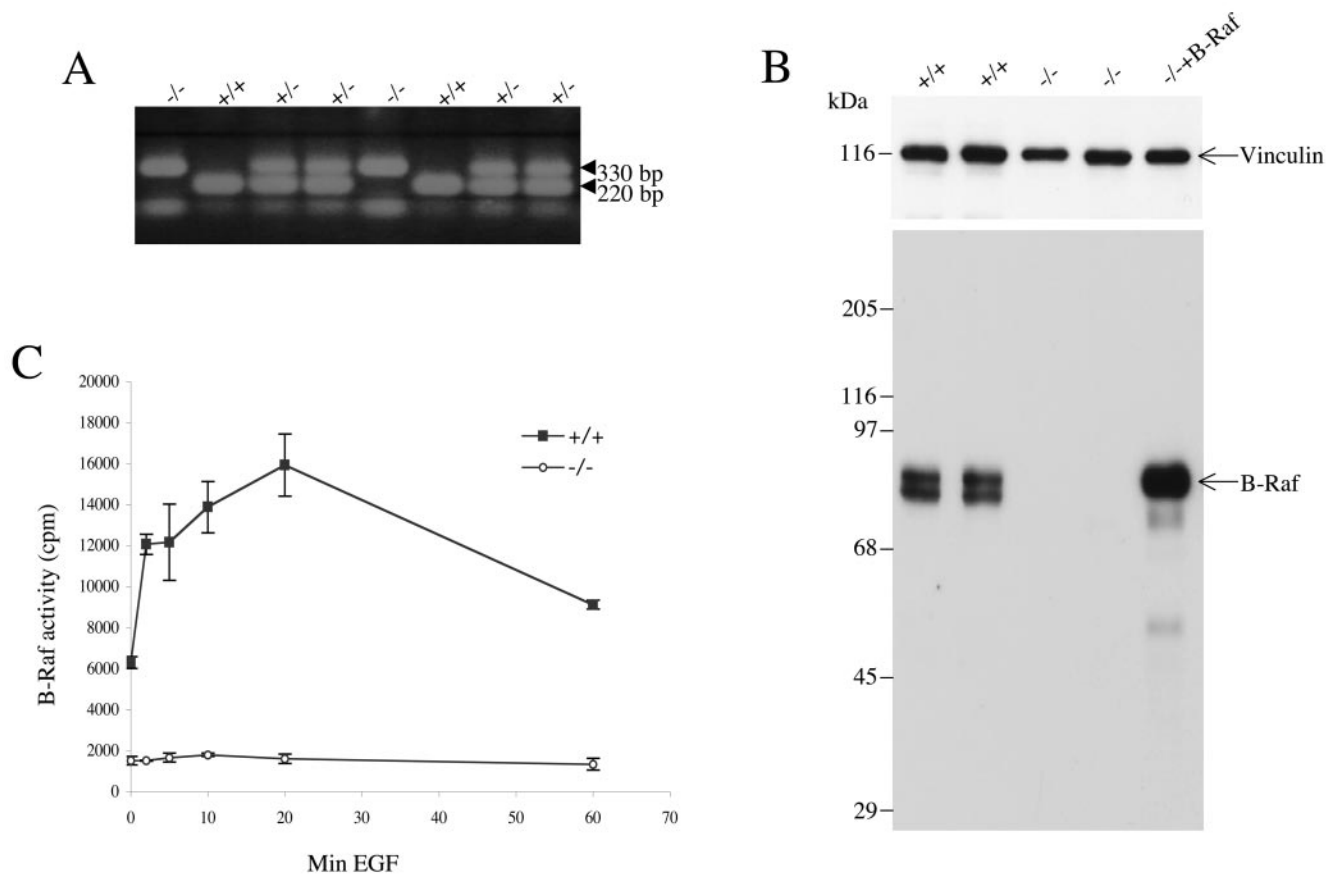


FIG. 1. (A) PCR genotyping of a typical litter from a *B-raf*^{+/-} intercross. DNA from embryo tail samples was genotyped by using the PCR strategy previously described (41) and analyzed by agarose gel electrophoresis. The 330-bp product is indicative of the mutant allele, whereas the 220-bp product is indicative of the wild-type allele. (B) Western blot showing the absence of B-Raf protein in *B-raf*^{-/-} cells. Lysates from two different clones of *B-raf*^{+/+} and *B-raf*^{-/-} cells and lysates from *B-raf*^{-/-} cells transfected with a human B-Raf cDNA were Western blotted and analyzed with an antibody specific for B-Raf (bottom panel). To control for protein loading, the blot was analyzed with an antibody for vinculin (top panel). (C) B-Raf kinase assay of *B-raf*^{+/+} and *B-raf*^{-/-} cells following EGF stimulation. *B-raf*^{+/+} and *B-raf*^{-/-} immortalized MEFs were serum starved and then stimulated with EGF over a time course of 0 to 60 min. Protein lysates were generated, and B-Raf activity was measured by using a kinase immunocomplex cascade assay (24). As expected, no B-Raf kinase activity was detected in *B-raf*^{-/-} cells. Error bars indicate standard deviations.

levels of phospho-ERK in *B-raf*^{-/-} cells, despite the presence of normal levels of total ERK1/2. However, the levels of phospho-ERK varied somewhat between experiments and between cell lines. At best, the levels of phospho-ERK2 in *B-raf*^{-/-} cells reached 40% the levels of phospho-ERK2 in *B-raf*^{+/+} cells. However, on many occasions, we found no detectable ERK1/2 phosphorylation in *B-raf*^{-/-} cells following stimulation of the cells.

***B-raf*^{-/-} MEFs have increased motility.** To assess the motility characteristics of MEFs, these cells were plated on fibronectin-treated plates and allowed to reach confluence. Wounding assays were performed by scraping wounds into the confluent monolayers and monitoring the migration of cells into the wounds by photographing the samples at regular intervals. Cells of all genotypes closed the wound by 20 h. While there was a degree of variability between MEFs of the same genotype, all *B-raf*^{-/-} cells migrated faster than *B-raf*^{+/+} cells (Fig. 3A). To quantitate movement into the wounds, changes in wound areas were measured (Fig. 3B). *B-raf*^{-/-} cells achieved 100% wound closure by 12 h, at which point *B-raf*^{+/+} cells had achieved only approximately 60% closure. This result

indicates that *B-raf*^{-/-} cells migrate approximately 1.7 times faster than *B-raf*^{+/+} cells.

To further assess motility, transmigration assays were performed by placing *B-raf*^{-/-} and *B-raf*^{+/+} cells in Boyden chambers. Movement of the cells across the chambers from serum-free medium to complete medium was measured following 5 h of incubation. The number of cells that transmigrated was quantitated for each cell line (see Materials and Methods). These assays were performed three times for three different MEFs of each genotype. Pooled data for all experiments are shown in Fig. 3C. The data are consistent with the wounding assay data, showing that *B-raf*^{-/-} cells migrate approximately 1.5 times faster than *B-raf*^{+/+} cells.

Changes in cell spreading and surface integrin expression for *B-raf*^{-/-} cells. Increased motility may be associated with the up-regulation of fibronectin-binding integrins at the cell surface which, in turn, may influence the rate of cell spreading. To investigate this possibility, we measured the surface expression of the two major fibronectin-binding integrins expressed in MEFs—the $\alpha 5\beta 1$ and $\alpha \beta 3$ heterodimers—by using the method described in Materials and Methods. The surface ex-

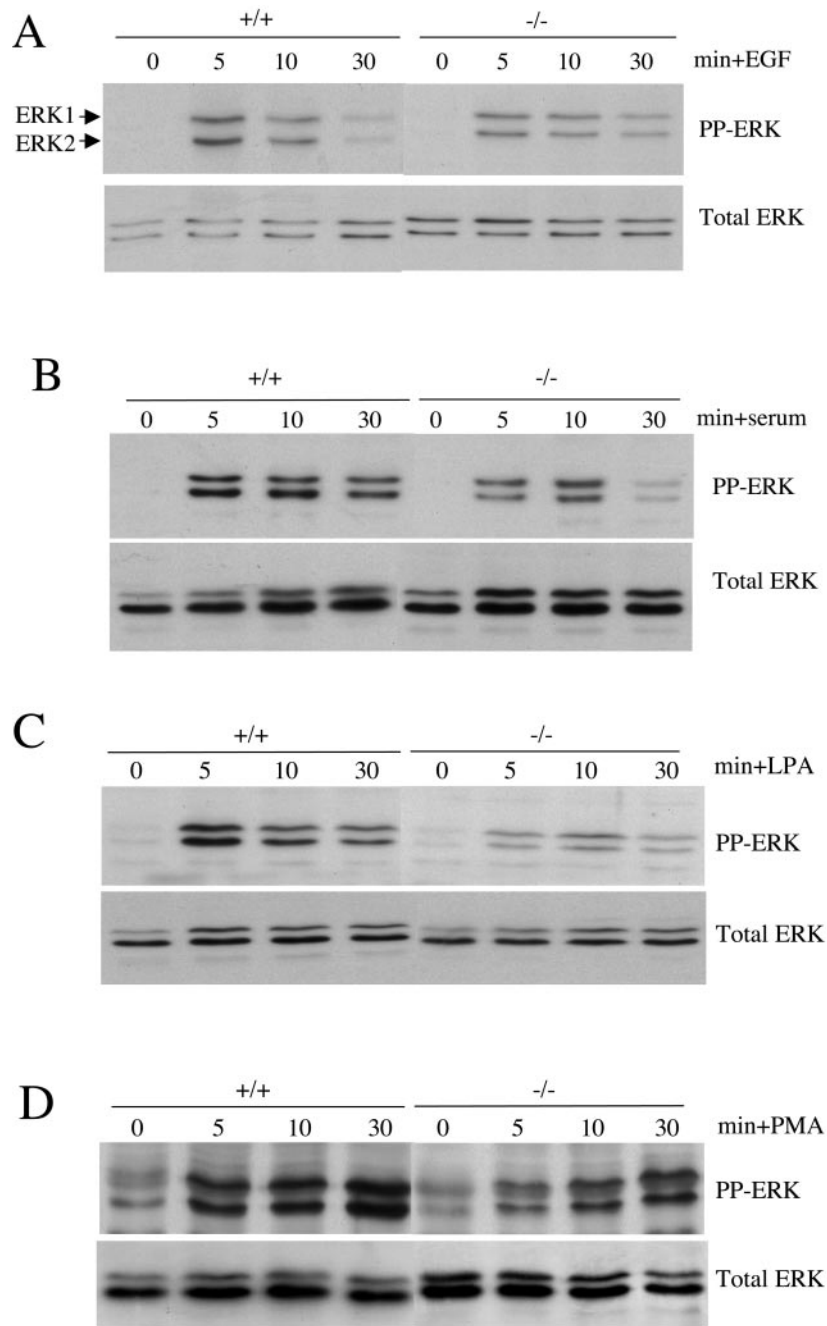


FIG. 2. Analysis of ERK phosphorylation in *B-raf*^{+/+} and *B-raf*^{-/-} MEFs. Primary MEFs were serum starved and then stimulated with EGF (A), 10% serum (B), LPA (C), or PMA (D) for the times indicated. Protein lysates were prepared and analyzed with an antibody for phospho-ERK (PP-ERK) (top panels) or total ERK (bottom panels). Experiments were repeated several times for clones of each genotype, and representative Western blots are shown. Levels of phospho-ERK were reduced in *B-raf*^{-/-} MEFs following treatment with all stimuli.

pression of $\alpha 5\beta 1$ was clearly unchanged by disruption of *B-raf*. However, the expression of $\alpha v\beta 3$ was reduced by $\approx 50\%$ (Fig. 4A). To confirm the integrity of immunologically isolated material, immunologically isolated samples were analyzed by SDS-PAGE under nonreducing conditions followed by Western blotting. Consistent with the capture enzyme-linked immunosorbent assay data, the surface expression of $\alpha v\beta 3$ was lower in *B-raf*^{-/-} cells than in *B-raf*^{+/+} cells, while that of $\alpha 5\beta 1$ remained unchanged (Fig. 4B).

Vitronectin is a good ligand for $\alpha v\beta 3$, while fibronectin binds to both $\alpha 5\beta 1$ and $\alpha v\beta 3$. It is likely, therefore, that the reduced expression of $\alpha v\beta 3$ will result in attenuated cell spreading on vitronectin, while the normal level of $\alpha 5\beta 1$ in *B-raf*^{-/-} cells will be able to maintain cell spreading on fibronectin. To analyze this possibility, we allowed *B-raf*^{-/-} and *B-raf*^{+/+} cells to spread for 30 min or 1 h on plates coated with either vitronectin or fibronectin in the presence of PDGF-BB; then, the cells were fixed, and their spread areas were determined by using

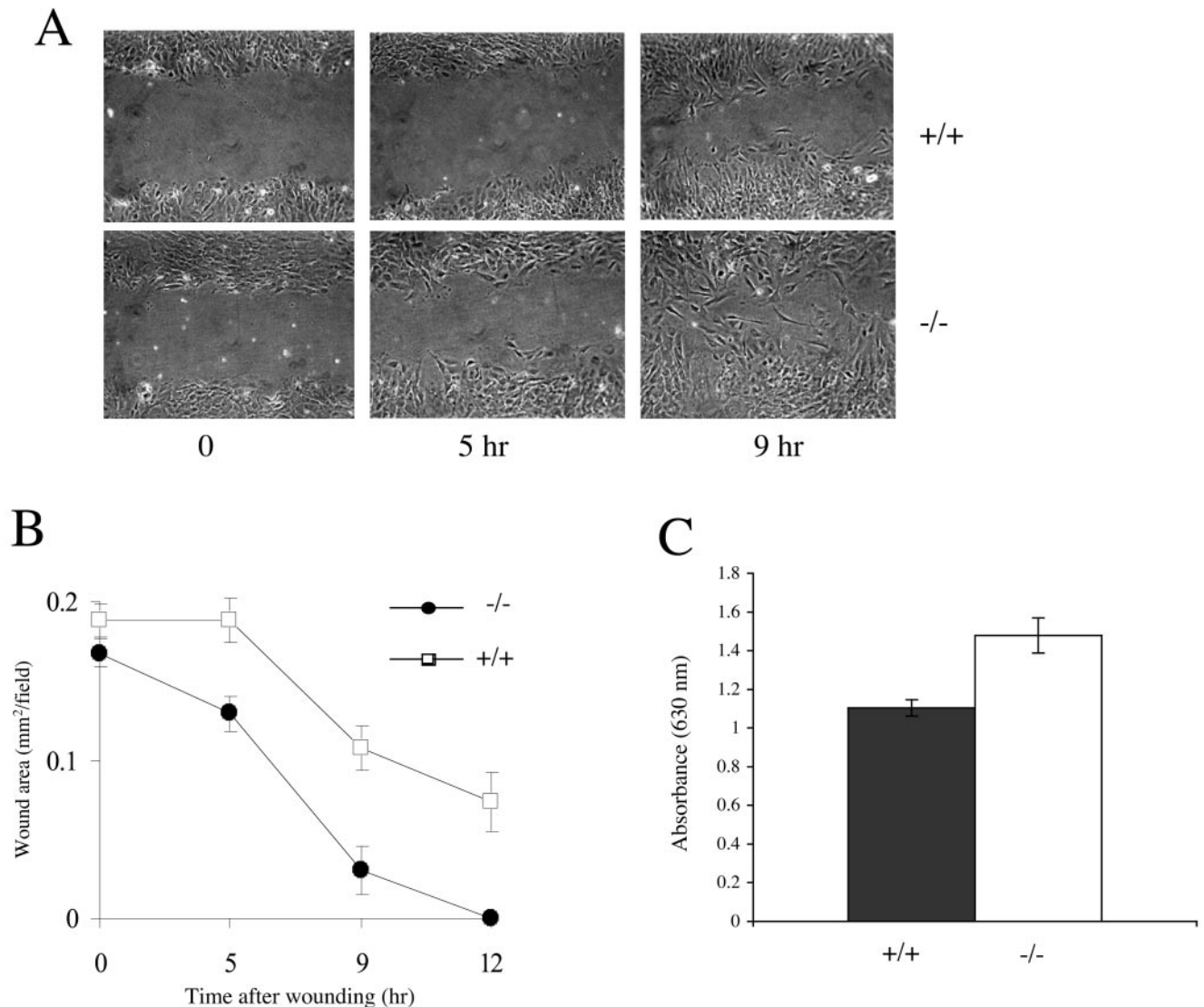


FIG. 3. Migration of *B-raf*^{-/-} and *B-raf*^{+/+} MEFs. (A) Wounding assay of *B-raf*^{+/+} (top panels) and *B-raf*^{-/-} primary MEFs (bottom panels). MEFs were plated on fibronectin and grown to confluence. A wound of approximately 0.5 mm was introduced into the monolayer, and the migration of cells was monitored by photographing at time points from 0 to 24 h. The 0-, 5-, and 9-h time points are shown for each cell line. (B) Quantitation of the wounding assay shown in panel A. For each cell line, the wound area was quantitated by using NIH Image software. Values are presented as means and standard deviations ($n = 10$ wounds). The data presented are typical of those obtained from three different experiments with three different cell lines of each genotype. (C) Transmigration assay of *B-raf*^{+/+} and *B-raf*^{-/-} MEFs. Primary MEFs were placed in Boyden chambers and allowed to transmigrate for 5 h as described in Materials and Methods. Cells that had transmigrated were stained with toluidine blue and quantified by measuring the absorbance at 630 nm. Assays were repeated three times with three different cell lines of each genotype. Data are presented as means and standard errors.

NIH Image software. After 30 min, no difference was observed in the abilities of *B-raf*^{-/-} and *B-raf*^{+/+} cells to spread on vitronectin (FIG. 4C). However, by 1 h, *B-raf*^{-/-} cells displayed a small but significant reduction in their ability to spread on vitronectin. In contrast, spreading on fibronectin was significantly increased by the disruption of *B-raf* (Fig. 4C). Similar data were obtained upon spreading of *B-raf*^{-/-} and *B-raf*^{+/+} cells on either matrix in serum-containing complete medium for 30 min (data not shown).

Analysis of actin stress fibers and focal adhesions in *B-raf*^{-/-} MEFs. Increased migration of a variety of cell types is accompanied by (1, 10) and indeed can be driven by (21)

increased expression of $\alpha v\beta 3$ integrin. Therefore, the reduced level of $\alpha v\beta 3$ that we found in *B-raf*^{-/-} cells is not consistent with their highly motile behavior and indicates that other factors must be contributing to this behavior. In cultured fibroblasts, high basal levels of actin stress fibers are known to be inhibitory to cell migration; the finding in *B-raf*^{-/-} cells of reduced levels of stress fibers might account for their increased motility. Therefore, we used immunofluorescence to analyze the integrity of the F-actin cytoskeleton of *B-raf*^{-/-} and *B-raf*^{+/+} cells. In all primary and immortalized cultures tested, *B-raf*^{+/+} MEFs displayed an array of thick bundled stress fibers (Fig. 5A and B and Fig. 6B and C). In contrast, the actin

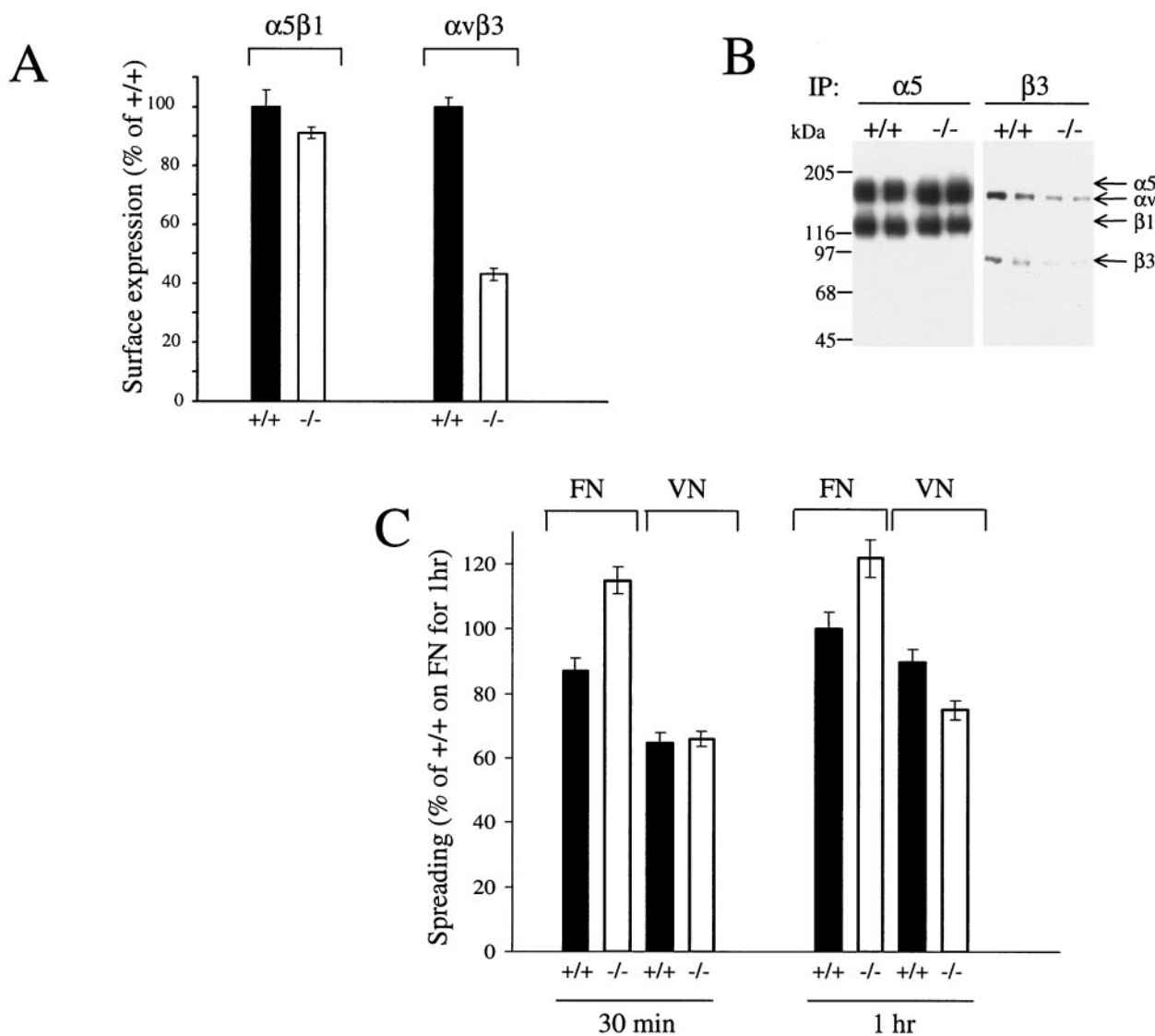


FIG. 4. Surface integrin expression and spreading assays. (A and B) Surface expression of $\alpha 5\beta 3$ and $\alpha 5\beta 1$ integrins. Cells were surface labeled and lysed, and integrins were captured by overnight incubation in microtiter wells coated with anti- $\alpha 5$ and anti- $\beta 3$ integrin monoclonal antibodies. Biotinylated integrins were detected by using peroxidase-conjugated streptavidin followed by a chromogenic reaction with *o*-phenylenediamine (A). To confirm the integrity of immunologically isolated material, samples were analyzed by SDS-PAGE under nonreducing conditions followed by Western blotting (B). IP, immunoprecipitation. (C) Spreading of cells on the extracellular matrix. MEFs in serum-free DMEM containing 10 ng of PDGF-BB/ml were spread on ligand-coated wells. Cells were allowed to attach for 30 min or 1 h, washed with PBS, fixed, and photographed. Cell areas were determined by using NIH Image software. FN, fibronectin; VN, vitronectin.

filaments in *B-raf*^{-/-} cells were notably less bundled and had an indistinct, less organized appearance (Fig. 5A and B and Fig. 6B and C). In addition, F-actin levels in *B-raf*^{-/-} and *B-raf*^{+/+} MEFs were quantitated. Cells were fixed, permeabilized, stained with FITC-phalloidin, and analyzed by FACS. F-actin levels were consistently reduced in all *B-raf*^{-/-} MEFs, compared to *B-raf*^{+/+} MEFs (Fig. 5B and C). However, the overall levels of expression of actin remained the same (Fig. 5D).

Immunofluorescence analysis showed that recruitment of paxillin and vinculin to focal adhesions in *B-raf*^{-/-} cells was normal (Fig. 5A), indicating that the observed reduction in the stress fiber background was insufficient to affect focal adhesion

assembly. We also analyzed the localization of total ERK in *B-raf*^{-/-} and *B-raf*^{+/+} cells by immunofluorescence. Consistent with previous data (9), *B-raf*^{+/+} cells displayed large focal adhesions containing ERK, and ERK was also aligned along actin stress fibers (Fig. 5B). However, recruitment of ERK to focal adhesions was reduced in *B-raf*^{-/-} cells, and ERK was no longer located along actin stress fibers (Fig. 5B). These data show that both ERK phosphorylation and localization are disrupted as a result of the *B-raf* knockout mutation.

An abnormal actomyosin contractile apparatus is not associated with decreased MLC₂₀ phosphorylation in *B-raf*^{-/-} MEFs. Klemke et al. (19) showed that both ERK1 and ERK2 are able to directly phosphorylate MLCK, leading to enhanced

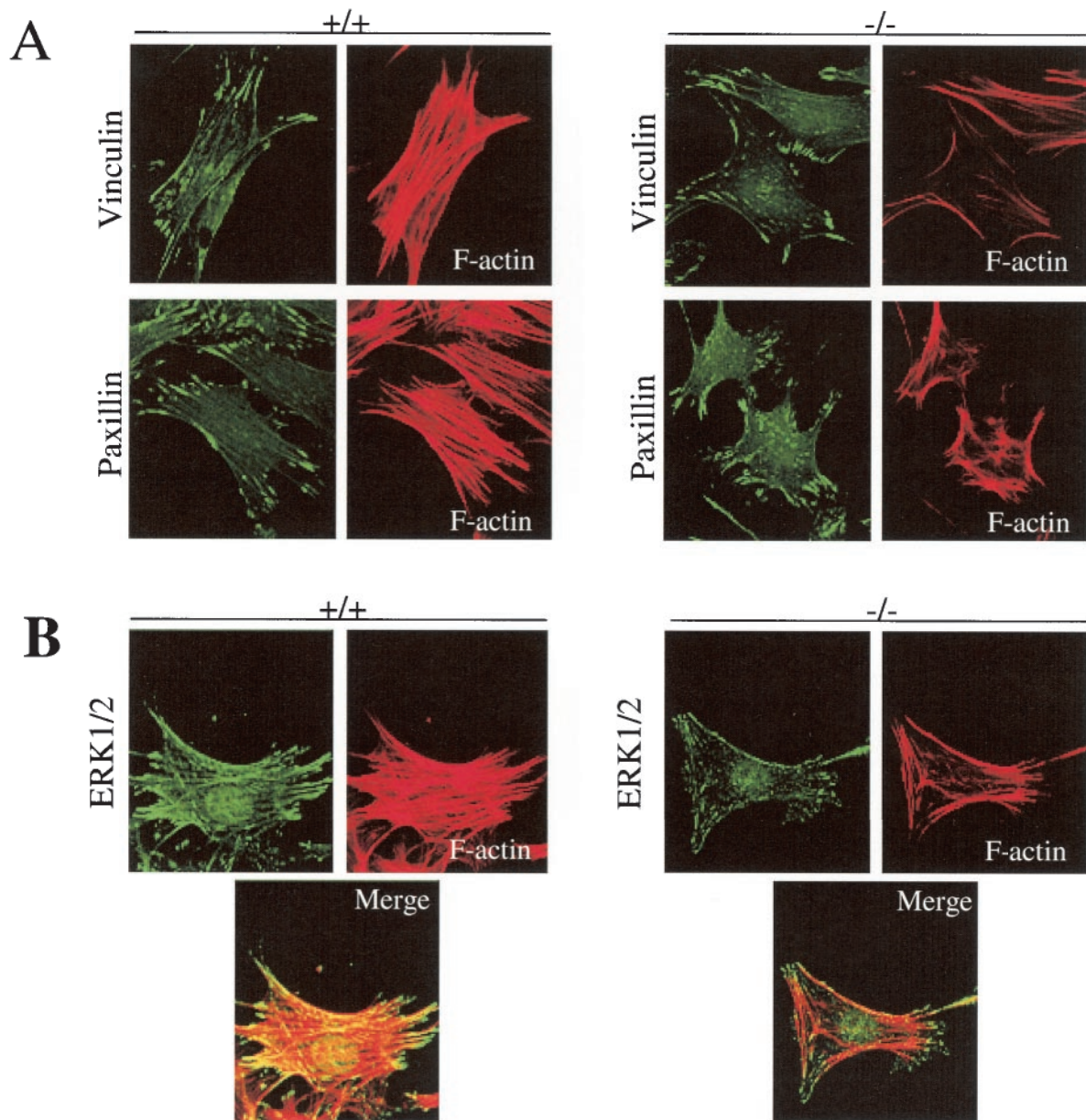


FIG. 5. Analysis of focal adhesions and the actin cytoskeleton. (A) Immunofluorescence analysis of *B-raf*^{+/+} and *B-raf*^{-/-} MEFs with antibodies for vinculin (top panels) or paxillin (bottom panels). Secondary antibodies conjugated to FITC were used. Typical examples of representative cells are shown. *B-raf*^{-/-} MEFs contain large vinculin- and paxillin-containing focal adhesions similar to those in *B-raf*^{+/+} cells (left panels). Cells were counterstained with Texas Red-phalloidin to detect the actin cytoskeleton (right panels). All *B-raf*^{-/-} cells contained an abnormal actin cytoskeleton. The stress fibers are notably less bundled and less well defined. (B) Immunofluorescence analysis of ERK1/2 localization. ERK1/2 was detected with an ERK-specific antibody followed by an FITC-conjugated secondary antibody (top left panels). Cells were counterstained with Texas Red-phalloidin to detect the actin cytoskeleton (top right panels). Images were merged in Adobe Photoshop (bottom panels). The merged images show that ERK localization is disrupted in *B-raf*^{-/-} cells. (C and D) FACS analysis (C) and quantitation (D) of FITC-phalloidin staining of *B-raf*^{+/+} and *B-raf*^{-/-} MEFs. Primary MEFs were fixed, permeabilized, stained with FITC-phalloidin, and analyzed by FACS. Data were pooled from three primary cell lines of each genotype. Error bars indicate standard deviations. (E) Coomassie blue staining of SDS-polyacrylamide gel showing normal levels of actin in *B-raf*^{-/-} lysates compared to *B-raf*^{+/+} lysates.

MLC phosphorylation. Therefore, it seems likely that B-Raf promotes contractility via ERK that acts to promote the phosphorylation of MLC₂₀. To investigate whether this pathway is disrupted in *B-raf*^{-/-} cells, we assessed the levels of MLC₂₀ phosphorylation. Protein lysates were generated from *B-raf*^{+/+} and *B-raf*^{-/-} MEFs, Western blotted, and analyzed with an antibody for Thr18/Ser19 phospho-MLC₂₀. While some vari-

ability was observed in the levels of MLC₂₀ phosphorylation between different primary MEFs, there was no consistent difference in the levels of MLC₂₀ phosphorylation between *B-raf*^{+/+} and *B-raf*^{-/-} cells (Fig. 6A). To further investigate MLC₂₀ phosphorylation, we used the Thr18/Ser19 phospho-MLC₂₀ antibody in an immunofluorescence analysis of immortalized (Fig. 6B) and primary (Fig. 6C) *B-raf*^{+/+} and *B-raf*^{-/-}

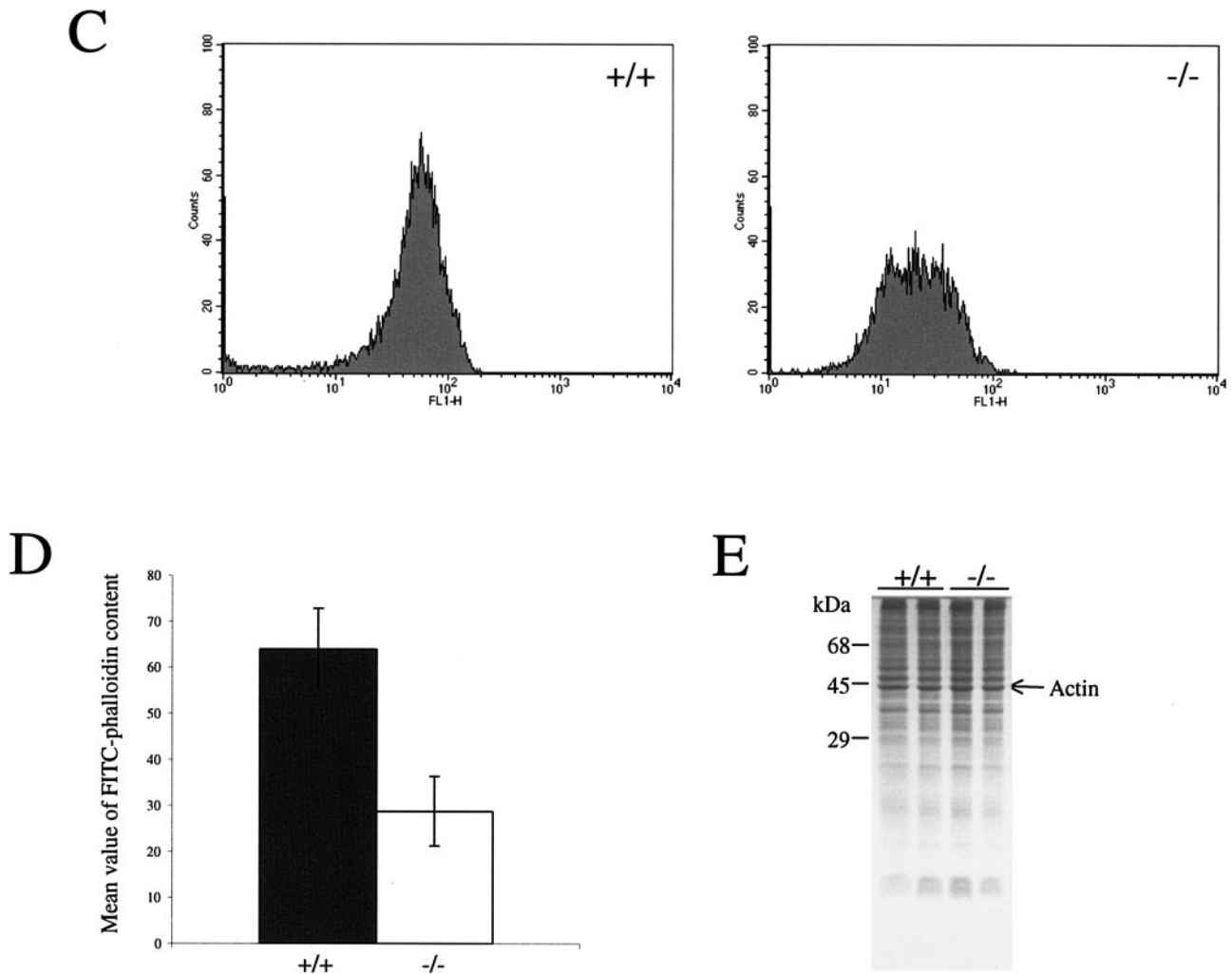


FIG. 5—Continued.

cells. In immortalized cells, while the overall level of phospho-MLC₂₀ clearly was not reduced, the distribution of phospho-MLC₂₀ was altered. In *B-raf*^{+/+} cells, phospho-MLC₂₀ was closely aligned with actin stress fibers. However, in *B-raf*^{-/-} cells, phospho-MLC₂₀ staining was uneven and contained within large, indistinct aggregates (Fig. 6B). Phospho-MLC₂₀ was more evenly distributed along actin stress fibers in *B-raf*^{-/-} primary MEFs than in *B-raf*^{-/-} immortalized MEFs, but it showed a slightly less regular distribution in *B-raf*^{-/-} primary MEFs than in *B-raf*^{+/+} primary MEFs and was certainly not reduced.

***B-raf*^{-/-} cells have reduced levels of ROCKII and phospho-ADF/cofilin.** The similar levels of MLC₂₀ phosphorylation in *B-raf*^{+/+} and *B-raf*^{-/-} cells suggest that the ERK-MLCK-MLC axis is not disrupted as a consequence of the *B-raf* knockout mutation. Therefore, to account for the observed reduction in the stress fiber background, we analyzed the Rho kinase-LIMK-cofilin pathway, which is known to be a major pathway in the control of F-actin levels within the cell. Protein lysates were generated from *B-raf*^{+/+} and *B-raf*^{-/-} primary MEFs and Western blotted with antibodies for ROCKI and ROCKII. No difference was observed in the levels of expression of ROCKI

in *B-raf*^{-/-} and *B-raf*^{+/+} cells. However, there was a clear and consistent decrease in the levels of expression of ROCKII in all *B-raf*^{-/-} primary MEFs compared to *B-raf*^{+/+} primary MEFs (Fig. 7A). Quantitative Western blotting indicated that ROCKII levels were reduced by two- to threefold in *B-raf*^{-/-} cells compared to *B-raf*^{+/+} cells.

Decreased levels of ROCKII in *B-raf*^{-/-} cells might be expected to lead to decreased levels of Ser3 phosphocofilin and thus to an increase in its depolymerizing activity and decreased levels of F-actin. To test this possibility, *B-raf*^{-/-} cells and *B-raf*^{+/+} cells were serum starved for 30 min and then treated with EGF over a time course of 0 to 20 min; Ser3 phosphocofilin levels were determined by Western blotting with a phosphospecific antibody. To control for protein loading, the samples were also Western blotted with antibodies detecting both phosphorylated cofilin and nonphosphorylated cofilin. In *B-raf*^{+/+} cells, the level of phosphocofilin in unstimulated cells was barely detectable but was increased by approximately 10-fold following treatment with EGF and was sustained for the length of the time course (Fig. 7B). In contrast, in *B-raf*^{-/-} cells, following stimulation with EGF, the level of phosphocofilin was reduced by approximately twofold and remained low

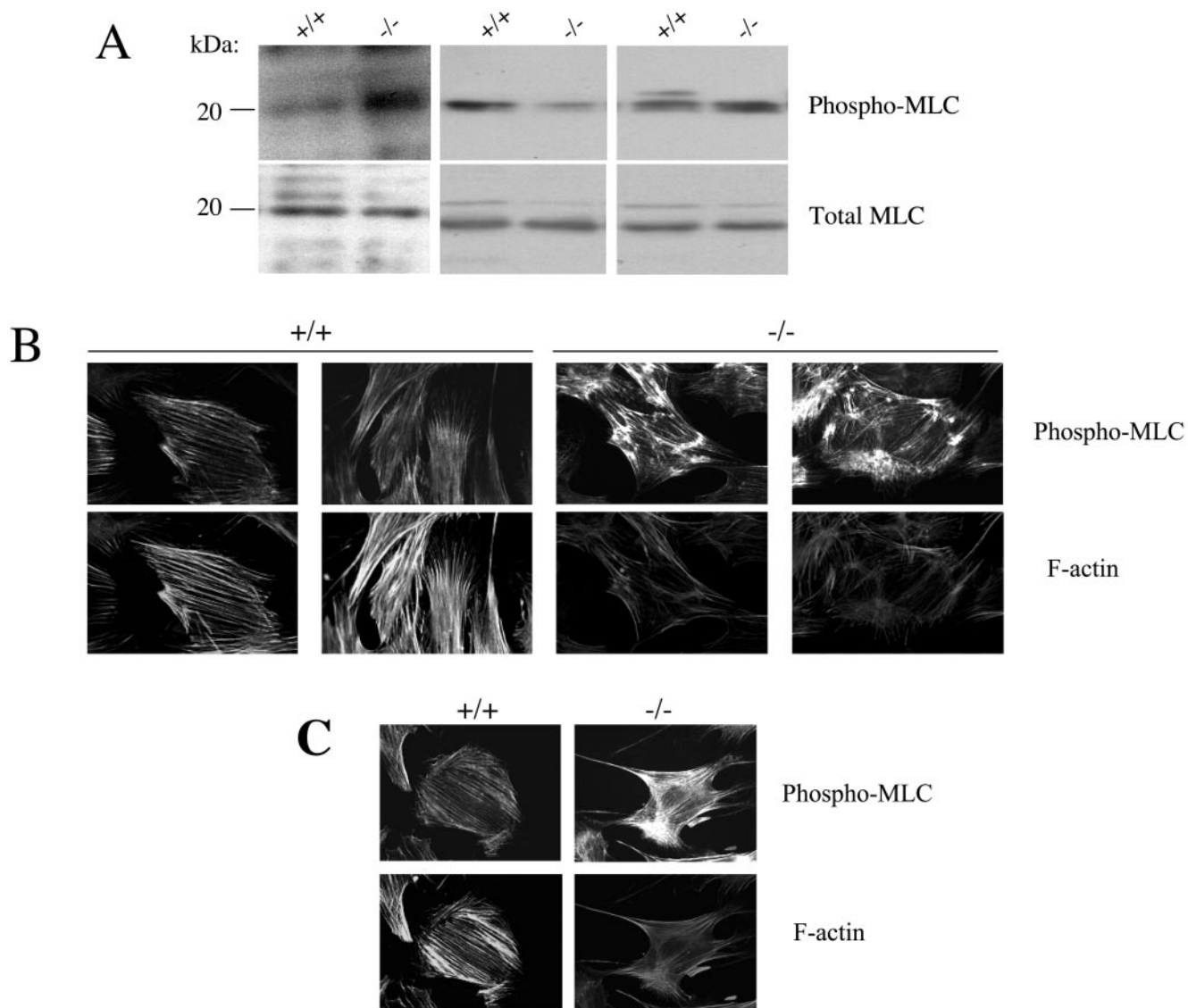


FIG. 6. (A) Western blot analysis of phospho-MLC in *B-raf*^{+/+} and *B-raf*^{-/-} MEFs. Three different primary MEF cell lines of each phenotype were refed with complete medium, and protein lysates were prepared. Western blot analysis was performed with an antibody that detects phospho-MLC₂₀ on Thr18/Ser19. To control for protein loading, blots were analyzed with an antibody for total MLC₂₀. While there was some variability in the level of phospho-MLC between individual MEFs, there was no consistent difference between *B-raf*^{-/-} and *B-raf*^{+/+} MEFs. (B) Immunofluorescence analysis of phospho-MLC and actin in *B-raf*^{+/+} and *B-raf*^{-/-} immortalized MEFs. (C) Immunofluorescence analysis of phospho-MLC and actin in *B-raf*^{+/+} and *B-raf*^{-/-} primary MEFs. Typical examples of representative cells are shown. While the overall level of phospho-MLC staining was no different, phospho-MLC was abnormally distributed and clumped. This pattern was more noticeable in immortalized cells (B) than in primary cells (C).

for the length of the time course (Fig. 7B). Levels of phosphocofilin were also analyzed following 10 min of treatment with the same agonists as those used to investigate ERK phosphorylation levels, namely, EGF, serum, LPA, and PMA. Following treatment with all stimuli, levels of phosphocofilin were increased far more in *B-raf*^{+/+} cells than in *B-raf*^{-/-} cells (Fig. 7C).

Defects in stress fiber assembly can be rescued by the overexpression of LIMK in *B-raf*^{-/-} cells and by the reexpression of B-Raf. To confirm that defects in a B-Raf-ROCKII-LIMK-cofilin pathway truly account for the abnormal phenotype of *B-raf*^{-/-} cells, we rescued the defect by expressing B-Raf, CA-MEK, and LIMK. Two different *B-raf*^{-/-} immortalized

MEF clones were transfected with vectors expressing Myc-tagged human B-Raf, CA-MEK with the S217E and S221E mutations, and HA-tagged full-length LIMK or a control vector expressing GFP. Using a Nucleofector, we achieved transfection frequencies of 80 to 90% with all vectors (Fig. 8C; GFP transfection). Following transfection, the transfected cells were used to seed tissue culture plates. After 24 h, they were placed in serum-free medium for 30 min. They were then serum stimulated for 10 min. Protein lysates were generated from serum-starved and serum-stimulated samples and analyzed by Western blotting with an antibody for Ser3 phosphocofilin (Fig. 8A). Cells transfected with the GFP vector demonstrated the

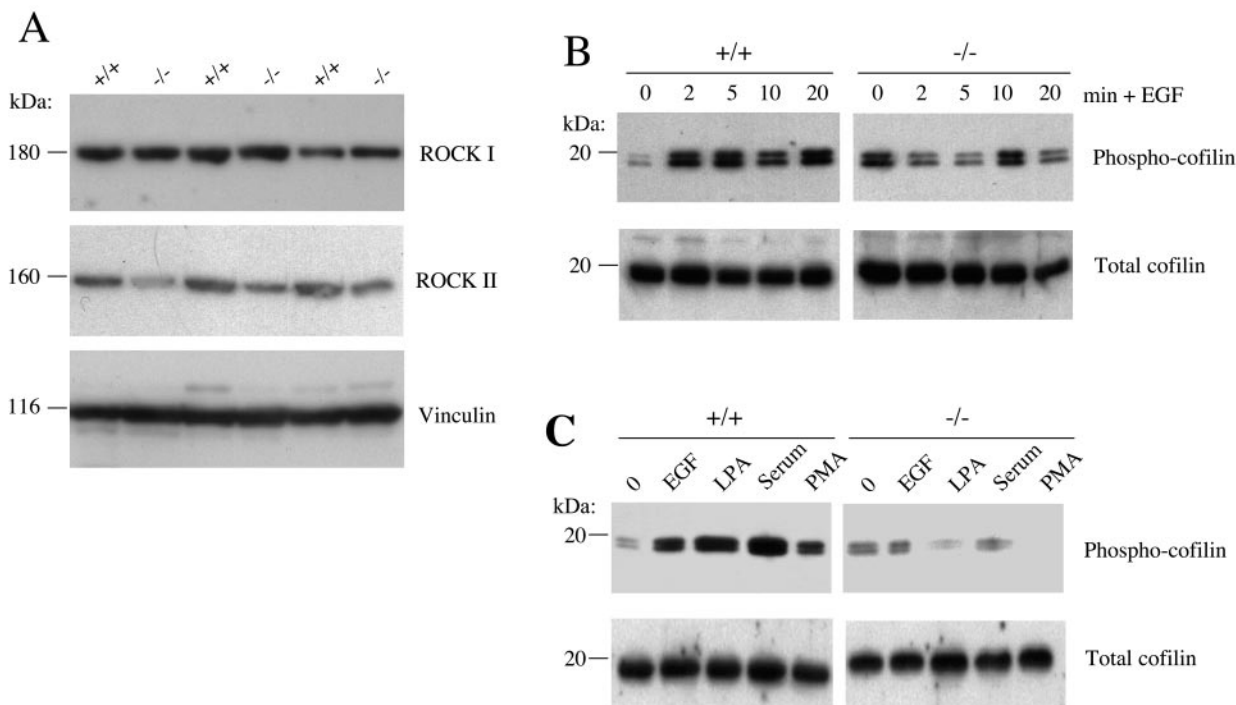


FIG. 7. (A) Western blot analysis of ROCKI and ROCKII expression levels in *B-raf*^{+/+} and *B-raf*^{-/-} primary MEFs. Three different primary MEF cell lines of each phenotype were refed with complete medium, and protein lysates were prepared. Western blot analysis was performed with an antibody that detects ROCKI (top panel) or ROCKII (middle panel). To control for protein loading, blots were analyzed with an antibody for vinculin. There was no difference in the levels of expression of ROCKI in the different cell lines, but ROCKII levels were consistently reduced in all *B-raf*^{-/-} cell lines. (B and C) Western blot analyses of phosphocofilin levels in *B-raf*^{+/+} and *B-raf*^{-/-} primary MEFs. (B) MEFs were serum starved and then stimulated with EGF over a time course of 0 to 20 min. (C) MEFs were serum starved and then stimulated with EGF, LPA, serum, or PMA for 10 min. Phosphocofilin levels were reduced in *B-raf*^{-/-} cells following treatment with all stimuli.

expression of phosphocofilin at levels similar to those seen in untransfected *B-raf*^{-/-} cells. However, for both *B-raf*^{-/-} clones, the expression of B-Raf, CA-MEK, or LIMK led to the restoration of Ser3 phosphocofilin expression following serum stimulation to levels similar to those seen in *B-raf*^{+/+} cells (Fig. 8A).

The two different *B-raf*^{-/-} immortalized clones then were transfected with the B-Raf, CA-MEK, and GFP vectors. At 24 h posttransfection, cells were serum starved for 30 min and then stimulated with serum for 10 min. Protein lysates were generated from serum-stimulated samples and analyzed by Western blotting with antibodies for ROCKII, B-Raf, and phospho-ERK1/2 (Fig. 8B). To control for protein loading, blots were incubated with an antibody for total ERK. Cells transfected with the GFP vector demonstrated the expression of ROCKII and the induction of phospho-ERK at levels similar to those seen in untransfected *B-raf*^{-/-} cells. However, as expected, transfection of cells with the B-Raf vector or the CA-MEK vector led to the concomitant restoration of phospho-ERK and ROCKII expression to levels similar to those seen in *B-raf*^{+/+} cells (Fig. 8B).

The actin cytoskeleton of the transfected cells was analyzed by immunofluorescence (Fig. 8C). Transfected cells were used to seed fibronectin-coated coverslips and were analyzed at 24 or 48 h posttransfection. Untransfected *B-raf*^{-/-} cells and *B-raf*^{-/-} cells transfected with the control GFP vector retained the appearance of a collapsed actin cytoskeleton with disorga-

nized stress fibers (Fig. 8C). In contrast, following transfection with the LIMK vector, the actin cytoskeleton of the *B-raf*^{-/-} cells reverted to an appearance similar to that of the actin cytoskeleton of *B-raf*^{+/+} cells. In B-Raf and CA-MEK transfections, rescue of the phenotype was observed after transfection for 24 h with both B-Raf and CA-MEK vectors (Fig. 8C). However, at 48 h posttransfection, the prolonged expression of B-Raf and CA-MEK led to the acquisition of a phenotype similar to that of a transformed cell (Fig. 8C).

DISCUSSION

A number of in vitro assays combined with kinase immunocomplex assays for endogenous Raf proteins suggested that B-Raf is the strongest MEK/ERK activator of the three mammalian Raf isoforms in several cell types (14, 16, 24, 33). However, this suggestion has not yet been confirmed by methods that down-regulate or inactivate B-Raf. In this report, we show that a knockout mutation of the *B-raf* gene in MEFs leads to the down-regulation of ERK1/2 phosphorylation by at least 60%. ERK1/2 phosphorylation is reduced to this level following treatment with a range of extracellular stimuli, including agents that operate through receptor tyrosine kinases (EGF) and agents that operate through G-coupled receptors (LPA). The fact that ERK1/2 phosphorylation is also reduced in response to phorbol ester stimulation provides support for the view that Raf activity is required for protein kinase C-mediated

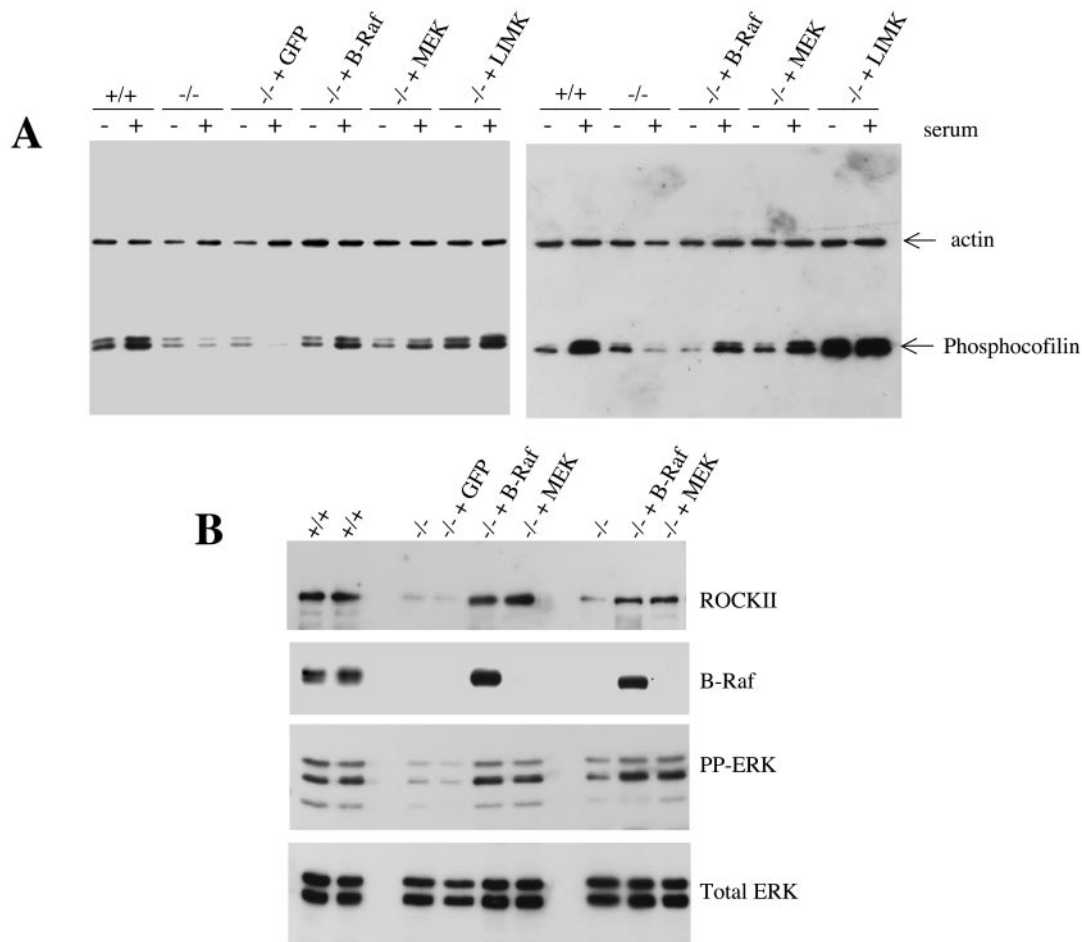


FIG. 8. Rescue of the *B-raf*^{-/-} phenotype by the expression of B-Raf, CA-MEK, and LIMK. (A) Restoration of Ser3 phosphocofilin levels. Two different *B-raf*^{-/-} clones were transfected with a vector expressing GFP, Myc-tagged B-Raf, CA-MEK, or HA-tagged LIMK. At 24 h posttransfection, cells were serum starved for 30 min and then stimulated with serum for 10 min. Protein lysates were generated from serum-starved and serum-stimulated cells, Western blotted, and analyzed with the Ser3 phosphocofilin antibody. To control for protein loading, blots were analyzed with an antibody for actin. For both *B-raf*^{-/-} clones, the expression of B-Raf, CA-MEK, and LIMK restored phosphocofilin levels to the levels observed in wild-type cells following serum stimulation. (B) Restoration of ROCKII and phospho-ERK expression levels. Two different *B-raf*^{-/-} clones were transfected with a vector expressing GFP, Myc-tagged B-Raf, or CA-MEK. At 24 h posttransfection, cells were serum starved for 30 min and then stimulated with serum for 10 min. Lysates were generated from serum-stimulated cells, Western blotted, and analyzed with an antibody for B-Raf, phospho-ERK (PP-ERK), or ROCKII. To control for protein loading, blots were analyzed with an antibody for total ERK. For both *B-raf*^{-/-} clones, transfection with the vectors expressing B-Raf and CA-MEK restored the level of expression of ROCKII and the induction of ERK1/2 phosphorylation to levels similar to those in wild-type cells. (C) Immunofluorescence analysis of *B-raf*^{+/+} cells, *B-raf*^{-/-} cells, and *B-raf*^{-/-} cells transfected with a vector expressing GFP, B-Raf, CA-MEK, or LIMK. Cells were transfected with the various vectors and used to seed fibronectin-coated coverslips at 24 h posttransfection for immunofluorescence analysis. For the B-Raf and CA-MEK transfections, cells were also used to seed coverslips at 48 h posttransfection. *B-raf*^{+/+} cells and *B-raf*^{-/-} cells transfected with the GFP vector were stained with Texas Red-phalloidin. Cells transfected with the vector expressing B-Raf, CA-MEK, or LIMK were stained with an antibody for the Myc tag, phospho-MEK, or the HA tag, respectively. Staining was detected with FITC-coupled secondary antibodies, and then the cells were counterstained with Texas Red-phalloidin. For the transfected cells, images detected through the FITC and Texas red channels were photographed independently and then merged in Adobe Photoshop. Merged images are shown.

ERK activation, as previously indicated (23, 37). Although ERK phosphorylation is reduced by at least 60% in *B-raf*^{-/-} cells, a significant level of ERK phosphorylation remains. It is not certain what this other MEK kinase activity is. It is unlikely to be due to an up-regulation of Raf-1 or A-Raf activities, since previous studies showed that the activities of both of these isoforms are decreased, not increased, in *B-raf*^{-/-} MEFs following stimulation with EGF (11, 40).

$\alpha\beta 3$ is the integrin predominantly involved in engaging vitronectin, whereas $\alpha 5\beta 1$ is unable to bind to this matrix protein. Therefore, the reduced ability of *B-raf*^{-/-} cells to

spread on vitronectin likely is due to reduced levels of expression of $\alpha\beta 3$ at the cell surface (Fig. 4). Consistent with our data, previous studies showed that Raf/ERK activation in 3T3 cells leads to increased expression of $\beta 3$ integrin (42). *B-raf*^{-/-} cells are able to spread efficiently on fibronectin; this result is unsurprising, as the surface levels of $\alpha 5\beta 1$, a good ligand for fibronectin, are unaffected by the disruption of B-Raf. The observed increased spreading of *B-raf*^{-/-} cells on fibronectin may have been due to the disruption of actin stress fibers and the down-regulation of ROCKII signaling. Indeed, it is known that a reduction in the activity of pathways downstream of Rho



FIG. 8—Continued.

can lead to enhanced cell spreading (38). Additionally, the fact that *B-raf*^{-/-} cells spread effectively on fibronectin suggests that B-Raf does not significantly influence Rac-regulated pathways leading to lamellopodial extension, at least in MEFs, consistent with the increased motility of *B-raf*^{-/-} cells.

We have noted that the lack of active ERK in *B-raf*^{-/-} cells is associated with a range of defects, including increased apoptosis (C.A.P., unpublished data), but the most pronounced defect is increased cell motility associated with the collapsed actin cytoskeleton and the reduced F-actin content reported in the present study. Surprisingly, this defect is not associated

with a disruption in the activation of MLCK, as evidenced by normal levels of MLC₂₀ phosphorylation in *B-raf*^{-/-} cells. These data suggest that the residual level of ERK1/2 phosphorylation observed in these cells is sufficient to allow normal levels of MLC₂₀ phosphorylation. The distribution of phospho-MLC₂₀ within *B-raf*^{-/-} MEFs is somewhat abnormal, but this may be a consequence of the abnormal assembly of actin stress fibers. In addition, *B-raf*^{-/-} cells form normal vinculin- and paxillin-containing focal adhesions (Fig. 5). Diaphanous formins, such as mouse Diaphanous (mDia), are known to be required for the induction of focal adhesions by either Rho.GTP

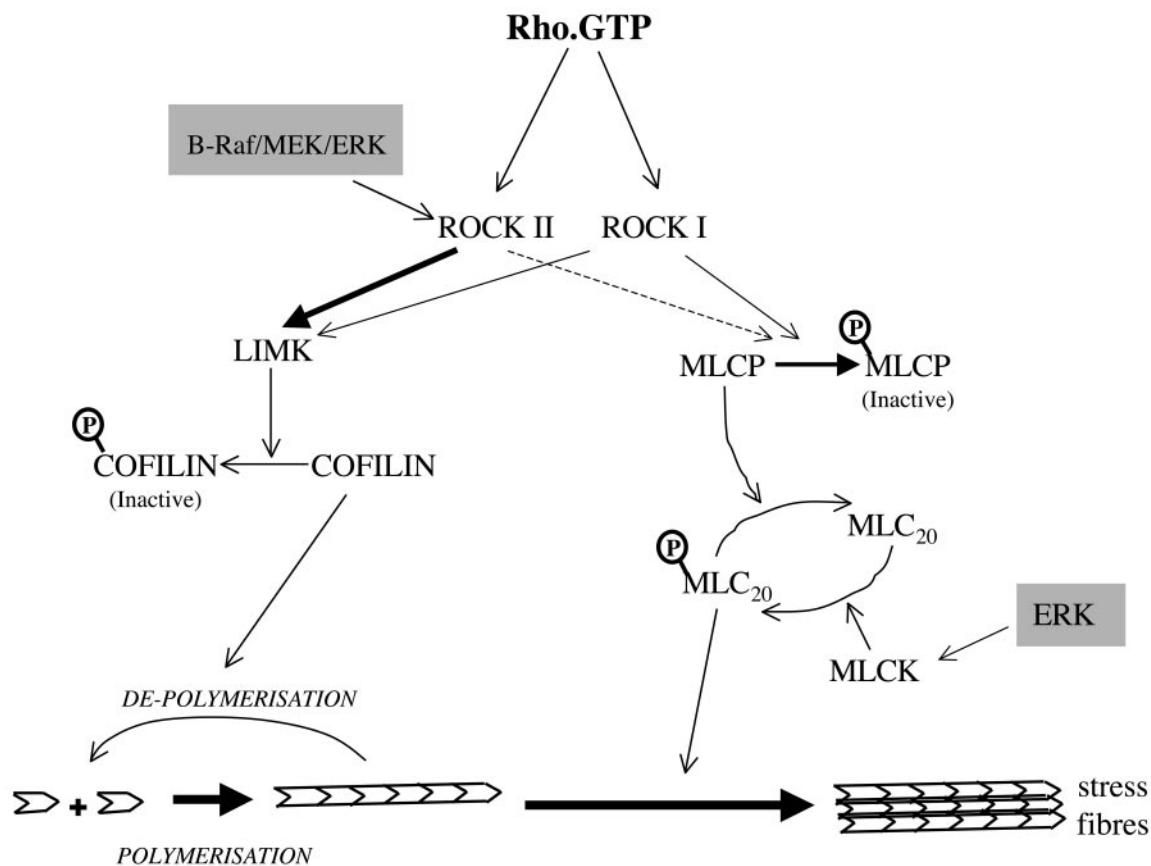


FIG. 9. Role of B-Raf/ERK in regulating Rho-activated pathways leading to actomyosin contraction. Actomyosin contraction is regulated by Rho, which acts via the Rho kinases (ROCKs). On the one hand, ROCK activates LIMK, which phosphorylates and inactivates the actin-depolymerizing protein cofilin. On the other hand, ROCK phosphorylates and inactivates MLCP, leading to increased MLC₂₀ phosphorylation and myosin ATPase activity, contraction of actin stress fibers, and cell movement. The points at which Raf/ERK may collaborate with Rho to enhance contractility are shaded. Klemke et al. (19) showed that ERKs activate MLCK, leading to enhanced MLC₂₀ phosphorylation. Our data are consistent with a role for B-Raf, through MEK/ERK, in specifically regulating the levels of ROCKII and thereby influencing signaling through the LIMK/cofilin axis but not through the MLCP/MLC₂₀ pathway.

or externally applied forces (34). Therefore, it seems unlikely that *B-raf*^{-/-} cells either have reduced levels of Rho.GTP or dysfunction in signaling from Rho.GTP to mDia, although it is conceivable that the spatial regulation of Rho activation is affected. Rather, our data provide strong evidence that the *B-raf* knockout mutation is associated with the uncoupling of Rho.GTP from stress fiber formation by selective reduction of the expression of the Rho effector ROCKII.

The Rho effectors, ROCKI and ROCKII, are known to have two functions in the regulation of actomyosin contractility (Fig. 9). First, they act to increase the phosphorylation of MLC by phosphorylating and inactivating MLC phosphatase (MLCP) (17). Second, they induce the activation of LIMK, thus inducing the phosphorylation of cofilin on Ser3 and inhibiting its actin-depolymerizing activity (43). The fact that the second function but not the first function is altered in *B-raf*^{-/-} cells identifies different roles for ROCKII with regard to these two effector pathways. Our data indicate that the maintenance of ROCKII expression levels is more critical for the LIMK/cofilin pathway than for the pathway leading to MLC₂₀ phosphorylation (Fig. 9). The mechanism by which B-Raf regulates selective ROCKII expression is not clear at this time. In oncogene-

transformed cells, it has been shown that constitutive MEK/ERK signaling alters ROCK and ROCKII protein expression but not mRNA levels, indicating that the effect is posttranscriptional (31); however, there may be a transcriptional component, as indicated by Zuber et al. (44). There are no reports of direct phosphorylation of ROCK by Raf or ERK, but it has been shown that B-Raf interacts with the PA28 α subunit of the 11S proteasome regulator in a yeast two-hybrid assay and when overexpressed in 293 cells, indicating that it may play a direct role in protein stability (15).

Serum response factor activity is sensed by cellular G-actin levels (36). However, despite the reduced F-actin levels and the unchanged total actin content of the *B-raf*^{-/-} cells, we saw no evidence of a reduction in the expression of serum response factor-inducible genes, such as those for vinculin and actin (Fig. 5 and 7). These findings suggest that the increased levels of active dephosphocofilin in *B-raf*^{-/-} cells may be sufficient to reduce the overall actin filament length but not to significantly raise cellular G-actin levels. However, an in-depth electron microscopic analysis would be needed to confirm this suggestion.

It is well established that the reduction of stress fiber for-

mation in fibroblastic cell types is correlated with increased motility. Indeed, previous studies from two leading laboratories indicated that cell transformation by oncogenic *v-src* (31) or Ras (35) promotes cell migration, at least in part, by effecting the disruption of actin stress fibers. Both of these groups have shown that *v-src* and Ras achieve this effect by chronically activating MEK/ERK, which in turn suppresses active ROCKI and ROCKII. We show that the normal functioning of the ROCKII/LIMK/cofilin axis clearly has a requirement for B-Raf. Taken together, our data and those from the studies just mentioned indicate that Raf/MEK/ERK signaling must be maintained at a moderate and appropriate level to ensure effective coupling between Rho and LIMK. Disruption of this balance, either by chronic elevation of MEK signaling or by genetic knockout of a key isoform of Raf, interferes with this pathway and leads to actin cytoskeleton disruption and increased cell migration. This situation is most clearly demonstrated in Fig. 8, where the reexpression of B-Raf causes the reversion of the actin cytoskeleton of *B-raf*^{-/-} cells to that of wild-type cells, whereas prolonged B-Raf and CA-MEK expression induces an actin cytoskeleton similar to that of transformed cells. In conclusion, our data suggest that the relationship between the Raf/MEK/ERK axis and cell migration likely is complex and that this complexity should be considered in the evaluation of B-Raf as a target for potential antimetastatic therapy.

ACKNOWLEDGMENTS

We are indebted to the Royal Society, Cancer Research UK, and The Wellcome Trust for their financial support.

We thank members of our laboratories for their invaluable support, particularly Kathryn Mercer, Melanie Banks, Alison Woods, Stuart Greene, Marnie Roberts, and Antonio Chiloehes. We are also grateful to J. Bamburg, M. Crow, A. Weeds, and V. Kotliansky for providing antibodies and Eric Sahai and Chris Marshall for providing the LIMK- and MEK-expressing vectors.

REFERENCES

- Albelda, S. M., S. A. Mette, D. E. Elder, R. Stewart, L. Damjanovich, M. Herlyn, and C. A. Buck. 1990. Integrin distribution in malignant melanoma: association of the beta 3 subunit with tumor progression. *Cancer Res.* **50**: 6757–6764.
- Bar-Sagi, D., and A. Hall. 2000. Ras and Rho GTPases: a family reunion. *Cell* **103**:227–238.
- Bos, J. L. 1989. ras oncogenes in human cancer: a review. *Cancer Res.* **49**:4682–4689.
- Cowley, S., H. Paterson, P. Kemp, and C. J. Marshall. 1994. Activation of MAP kinase kinase is necessary and sufficient for PC12 differentiation and for transformation of NIH 3T3 cells. *Cell* **77**:841–852.
- D'Angelo, G., and L. P. Adam. 2002. Inhibition of ERK attenuates force development by lowering myosin light chain phosphorylation. *Am. J. Physiol. Heart Circ. Physiol.* **282**:H602–H610.
- Davies, H., G. R. Bignell, C. Cox, P. Stephens, S. Edkins, S. Clegg, J. Teague, H. Woffendin, M. J. Garnett, W. Bottomley, N. Davis, E. Dicks, R. Ewing, Y. Floyd, K. Gray, S. Hall, R. Hawes, J. Hughes, V. Kosmidou, A. Menzies, C. Mould, A. Parker, C. Stevens, S. Watt, S. Hooper, R. Wilson, H. Jayatilake, B. A. Gusterson, C. Cooper, J. Shipley, D. Hargrave, K. Pritchard-Jones, N. Maitland, G. Chenevix-Trench, G. J. Riggins, D. D. Bigner, G. Palmieri, A. Cossu, A. Flanagan, A. Nicholson, J. W. Ho, S. Y. Leung, S. T. Yuen, B. L. Weber, H. F. Seigler, T. L. Darrow, H. Paterson, R. Marais, C. J. Marshall, R. Wooster, M. R. Stratton, and P. A. Futreal. 2002. Mutations of the BRAF gene in human cancer. *Nature* **417**:949–954.
- Dickson, B., and E. Hafen. 1994. Genetics of signal transduction in invertebrates. *Curr. Opin. Genet. Dev.* **4**:64–70.
- Downward, J. 2003. Targeting RAS signalling pathways in cancer therapy. *Nat. Rev. Cancer* **3**:11–22.
- Fincham, V. J., M. James, M. C. Frame, and S. J. Winder. 2000. Active ERK/MAP kinase is targeted to newly forming cell-matrix adhesions by integrin engagement and v-Src. *EMBO J.* **19**:2911–2923.
- Gehlsen, K. R., G. E. Davis, and P. Sriramarao. 1992. Integrin expression in human melanoma cells with differing invasive and metastatic properties. *Clin. Exp. Metastasis* **10**:111–120.
- Gomez, E., C. Pritchard, and T. P. Herbert. 2002. cAMP dependent protein kinase and Ca⁺⁺ influx through L-type voltage gated calcium channels mediate Raf independent activation of extracellular regulated kinase in response to glucagon like peptide-1 in pancreatic beta-cells. *J. Biol. Chem.* **277**:2.
- Hagemann, C., and U. R. Rapp. 1999. Isozyme-specific functions of Raf kinases. *Exp. Cell Res.* **253**:34–46.
- Hoshino, R., Y. Chatani, T. Yamori, T. Tsuruo, H. Oka, O. Yoshida, Y. Shimada, S. Ari-i, H. Wada, J. Fujimoto, and M. Kohno. 1999. Constitutive activation of the 41-/43-kDa mitogen-activated protein kinase signaling pathway in human tumors. *Oncogene* **18**:813–822.
- Huser, M., J. Luckett, A. Chiloehes, K. Mercer, M. Iwobi, S. Giblett, X. M. Sun, J. Brown, R. Marais, and C. Pritchard. 2001. MEK kinase activity is not necessary for Raf-1 function. *EMBO J.* **20**:1940–1951.
- Kalmes, A., C. Hagemann, C. K. Weber, L. Wixler, T. Schuster, and U. R. Rapp. 1998. Interaction between the protein kinase B-Raf and the alpha-subunit of the 11S proteasome regulator. *Cancer Res.* **58**:2986–2990.
- Kao, S., R. K. Jaiswal, W. Kolch, and G. E. Landreth. 2001. Identification of the mechanisms regulating the differential activation of the mapk cascade by epidermal growth factor and nerve growth factor in PC12 cells. *J. Biol. Chem.* **276**:18169–18177.
- Kawano, Y., Y. Fukata, N. Oshiro, M. Amano, T. Nakamura, M. Ito, F. Matsumura, M. Inagaki, and K. Kaibuchi. 1999. Phosphorylation of myosin-binding subunit (MBS) of myosin phosphatase by Rho-kinase in vivo. *J. Cell Biol.* **147**:1023–1038.
- Kimura, E. T., M. N. Nikiforova, Z. Zhu, J. A. Knauf, Y. E. Nikiforov, and J. A. Fagin. 2003. High prevalence of BRAF mutations in thyroid cancer: genetic evidence for constitutive activation of the RET/PTC-RAS-BRAF signaling pathway in papillary thyroid carcinoma. *Cancer Res.* **63**:1454–1457.
- Klemke, R. L., S. Cai, A. L. Giannini, P. J. Gallagher, P. de Lanerolle, and D. A. Cheresh. 1997. Regulation of cell motility by mitogen-activated protein kinase. *J. Cell Biol.* **137**:481–492.
- Kolch, W. 2001. To be or not to be: a question of B-Raf? *Trends Neurosci.* **24**:498–500.
- Li, X., B. Chen, S. D. Blystone, K. P. McHugh, F. P. Ross, and D. M. Ramos. 1998. Differential expression of av integrins in K1735 melanoma cells. *Invasion Metastasis* **18**:1–14.
- Luckett, J. C., M. B. Huser, N. Giagtzoglou, J. E. Brown, and C. A. Pritchard. 2000. Expression of the A-raf proto-oncogene in the normal adult and embryonic mouse. *Cell Growth Differ.* **11**:163–171.
- Marais, R., Y. Light, C. Mason, H. Paterson, M. F. Olson, and C. J. Marshall. 1998. Requirement of Ras-GTP-Raf complexes for activation of Raf-1 by protein kinase C. *Science* **280**:109–112.
- Marais, R., Y. Light, H. F. Paterson, C. S. Mason, and C. J. Marshall. 1997. Differential regulation of Raf-1, A-Raf, and B-Raf by oncogenic ras and tyrosine kinases. *J. Biol. Chem.* **272**:4378–4383.
- Marais, R., and C. J. Marshall. 1996. Control of the ERK MAP kinase cascade by Ras and Raf. *Cancer Surv.* **27**:101–125.
- Mason, C. S., C. J. Springer, R. G. Cooper, G. Superti-Furga, C. J. Marshall, and R. Marais. 1999. Serine and tyrosine phosphorylations cooperate in Raf-1 but not B-Raf activation. *EMBO J.* **18**:2137–2148.
- Mercer, K., A. Chiloehes, M. Huser, M. Kiernan, R. Marais, and C. Pritchard. 2002. ERK signalling and oncogene transformation are not impaired in cells lacking A-Raf. *Oncogene* **21**:347–355.
- Mikula, M., M. Schreiber, Z. Husak, L. Kucerova, J. Ruth, R. Wieser, K. Zatloukal, H. Beug, E. F. Wagner, and M. Baccarini. 2001. Embryonic lethality and fetal liver apoptosis in mice lacking the c-raf-1 gene. *EMBO J.* **20**:1952–1962.
- Papin, C., A. Denouel-Galy, D. Laugier, G. Calothy, and A. Eychene. 1998. Modulation of kinase activity and oncogenic properties by alternative splicing reveals a novel regulatory mechanism for B-Raf. *J. Biol. Chem.* **273**:24939–24947.
- Pawlak, G., and D. M. Helfman. 2002. MEK mediates v-Src-induced disruption of the actin cytoskeleton via inactivation of the Rho-ROCK-LIM kinase pathway. *J. Biol. Chem.* **277**:26927–26933.
- Pawlak, G., and D. M. Helfman. 2002. Post-transcriptional down-regulation of ROCKI/Rho-kinase through an MEK-dependent pathway leads to cytoskeleton disruption in Ras-transformed fibroblasts. *Mol. Biol. Cell* **13**:336–347.
- Pritchard, C. A., L. Bolin, R. Slattery, R. Murray, and M. McMahon. 1996. Post-natal lethality and neurological and gastrointestinal defects in mice with targeted disruption of the A-Raf protein kinase gene. *Curr. Biol.* **6**:614–617.
- Pritchard, C. A., M. L. Samuels, E. Bosch, and M. McMahon. 1995. Conditionally oncogenic forms of the A-Raf and B-Raf protein kinases display different biological and biochemical properties in NIH 3T3 cells. *Mol. Cell Biol.* **15**:6430–6442.
- Rivelino, D., E. Zamir, N. Q. Balaban, U. S. Schwarz, T. Ishizaki, S. Narumiya, Z. Kam, B. Geiger, and A. D. Bershadsky. 2001. Focal contacts as mechanosensors: externally applied local mechanical force induces growth of

- focal contacts by an mDia1-dependent and ROCK-independent mechanism. *J. Cell Biol.* **153**:1175–1186.
35. **Sahai, E., M. F. Olson, and C. J. Marshall.** 2001. Cross-talk between Ras and Rho signalling pathways in transformation favours proliferation and increased motility. *EMBO J.* **20**:755–766.
36. **Sotiropoulos, A., D. Gineitis, J. Copeland, and R. Treisman.** 1999. Signal-regulated activation of serum response factor is mediated by changes in actin dynamics. *Cell* **98**:159–169.
37. **Troppmair, J., J. T. Bruder, H. App, H. Cai, L. Liptak, J. Szeberenyi, G. M. Cooper, and U. R. Rapp.** 1992. Ras controls coupling of growth factor receptors and protein kinase C in the membrane to Raf-1 and B-Raf protein serine kinases in the cytosol. *Oncogene* **7**:1867–1873.
38. **Tsuji, T., T. Ishizaki, M. Okamoto, C. Higashida, K. Kimura, T. Furu-yashiki, Y. Arakawa, R. B. Birge, T. Nakamoto, H. Hirai, and S. Narumiya.** 2002. ROCK and mDia1 antagonize in Rho-dependent Rac activation in Swiss 3T3 fibroblasts. *J. Cell Biol.* **157**:819–830.
39. **Whitmarsh, A. J., and R. J. Davis.** 2000. A central control for cell growth. *Nature* **403**:255–256.
40. **Wojnowski, L., L. F. Stancato, A. C. Lerner, U. R. Rapp, and A. Zimmer.** 2000. Overlapping and specific functions of Braf and Craf-1 proto-oncogenes during mouse embryogenesis. *Mech. Dev.* **91**:97–104.
41. **Wojnowski, L., A. M. Zimmer, T. W. Beck, H. Hahn, R. Bernal, U. R. Rapp, and A. Zimmer.** 1997. Endothelial apoptosis in Braf-deficient mice. *Nat. Genet.* **16**:293–297.
42. **Woods, D., H. Cherwinski, E. Venetsanakos, A. Bhat, S. Gysin, M. Humbert, P. F. Bray, V. L. Saylor, and M. McMahon.** 2001. Induction of β 3-integrin gene expression by sustained activation of the Ras-regulated Raf-MEK-extracellular signal-regulated kinase signaling pathway. *Mol. Cell. Biol.* **21**:3192–3205.
43. **Yang, N., O. Higuchi, K. Ohashi, K. Nagata, A. Wada, K. Kangawa, E. Nishida, and K. Mizuno.** 1998. Cofilin phosphorylation by LIM-kinase 1 and its role in Rac-mediated actin reorganization. *Nature* **393**:809–812.
44. **Zuber, J., O. I. Tchernitsa, B. Hinzmann, A. C. Schmitz, M. Grips, M. Hellriegel, C. Sers, A. Rosenthal, and R. Schafer.** 2000. A genome-wide survey of RAS transformation targets. *Nat. Genet.* **24**:144–152.